

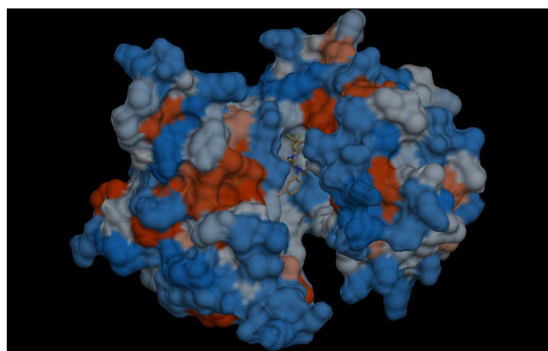
**This item is the archived peer-reviewed author-version of:**

Combined spectroscopic, DFT, TD-DFT and MD study of newly synthesized thiourea derivative

**Reference:**

Menon Vidya V., Mary Y. Sheena, Mary Y. Shyma, Panicker C. Yohannan, Bielenica Anna, Armaković Stevan, Armaković Sanja J., Van Alsenoy Christian.-  
Combined spectroscopic, DFT, TD-DFT and MD study of newly synthesized thiourea derivative  
Journal of molecular structure - ISSN 0022-2860 - 1155(2018), p. 184-195  
Full text (Publisher's DOI): <https://doi.org/10.1016/J.MOLSTRUC.2017.10.093>  
To cite this reference: <https://hdl.handle.net/10067/1478710151162165141>

Investigation of new thiourea derivative -  
1-(3-bromophenyl)-3-[3-(trifluoromethyl)phenyl]thiourea



ACCEPTED MANUSCRIPT

***Combined spectroscopic, DFT, TD-DFT and MD study of newly synthesized thiourea derivative***

Vidya V. Menon<sup>a,b</sup>, Sheena Mary Y<sup>c</sup>, Shyma Mary Y<sup>c</sup>, C. YohannanPanicker<sup>c</sup>, Anna Bielenica<sup>d</sup>,  
Stevan Armaković<sup>e,\*</sup>, Sanja J. Armaković<sup>f</sup>, Christian Van Alsenoy<sup>g</sup>

<sup>a</sup>Department of Physics, IES College of Engineering, Chittilappily, Thrissur, Kerala, India

<sup>b</sup>RD, Bharathiar University, Coimbatore, Tamilnadu, India

<sup>c</sup>Department of Physics, Fatima Mata National College, Kollam, Kerala, India

<sup>d</sup>Chair and Department of Biochemistry, Medical University of Warsaw, 02-097 Warszawa, Poland,

<sup>e</sup>University of Novi Sad, Faculty of Sciences, Department of Physics, Trg D. Obradovića 4, 21000 Novi Sad, Serbia

<sup>f</sup> University of Novi Sad, Faculty of Sciences, Department of Chemistry, Biochemistry and Environmental Protection, Trg D. Obradovića 3, 21000 Novi Sad, Serbia

<sup>g</sup>Department of Chemistry, University of Antwerp, Groenenborgerlaan 171, B-2020 Antwerp, Belgium

\*author for correspondence:

Dr. Stevan Armaković

Email: [stevan.armakovic@df.uns.ac.rs](mailto:stevan.armakovic@df.uns.ac.rs)

University of Novi Sad, Faculty of Sciences, Department of Physics

Trg Dositeja Obradovića 4, 21000 Novi Sad, Serbia

## Abstract

A novel thiourea derivative, 1-(3-bromophenyl)-3-[3-(trifluoromethyl)phenyl]thiourea (ANF-22) is synthesized and characterized by FTIR, FT-Raman and NMR spectroscopy experimentally and theoretically. A detailed conformational analysis of the title molecule has been conducted in order to locate the lowest energy geometry, which was further subjected to the detailed investigation of spectroscopic, reactive, degradation and docking studies by density functional theory (DFT) calculations and molecular dynamics (MD) simulations. Time dependent DFT (TD-DFT) calculations have been used also in order to simulate UV spectra and investigate charge transfer within molecule. Natural bond orbital analysis has been performed analyzing the charge delocalization and using HOMO and LUMO energies the electronic properties are analyzed. Molecular electrostatic potential map is used for the quantitative measurement of active sites in the molecule. In order to determine the locations possibly prone to electrophilic attacks we have calculated average local ionization energies and mapped them to the electron density surface. Further insight into the local reactivity properties have been obtained by calculation of Fukui functions, also mapped to the electron density surface. Possible degradation properties by the autoxidation mechanism have been assessed by calculations of bond dissociation energies for hydrogen abstraction. Atoms of title molecule with significant interactions with water molecules have been determined by calculations of radial distribution functions. The title compound can be a lead compound for developing new analgesic drug.

**Keywords:** Thiourea derivative; DFT; Local Ionization Energies (ALIE); Radial Distribution Functions (RDFs); Bond Dissociation Energies (BDE); Docking.

## 1. Introduction

Substituted thiourea derivatives have focused considerable attention due to their interesting pharmacological activities, including anticancer [1-3], antibacterial [1, 4, 5] and antiviral [6-8]. As the 5-HT<sub>2A</sub> receptor antagonists they produced a dose-dependent decrease in the number of DOI-evoked head-twitch responses and exerted both antinociceptive and anticonvulsant properties [5, 9-15]. On the other hand, it was well documented that thiourea-based compounds endowed with weakly deactivating halogen substituents at *meta*-and/or *para*-

position of the phenyl ring exerted considerable antimicrobial potency [1, 2]. The title 3-bromophenyl derivative, as the bacterial topoisomerase IV inhibitor, exhibited so far the strongest activity against Gram-positive cocci among all evaluated 3-(trifluoromethyl)phenylthioureas [1]. Inhibiting also the bacterial biofilm formation, had no impact on human normal cells viability and mortality [1]. Thiourea derivatives are versatile molecules which are capable of coordinating with metal ions and binding with biological targets to form stable complexes [2, 16, 17]. Oxygen, nitrogen and sulfur contribute in such bonding and increase the chances of thiourea derivatives binding with different biological receptors. The need for new chemotherapies for cancer and infectious diseases has motivated many researchers to use thiourea in combination with other moieties to design drugs for such diseases [18]. Imidazole is a versatile ring with paramount biological importance [19-22] which is evident from the fact that it constitutes skeleton of many commercial drugs like metronidazole (antimicrobial), imidazole (antifungal) drugs, cimetidine (histamine H<sub>2</sub>-receptor antagonist) and flumazenil (GABA<sub>A</sub> receptor antagonist). Imidazole polyamides constitute a highly active structural group which shows anti-cancerous properties by binding at DNA minor groove [23, 24]. Combining multiple pharmacophoric units into a single molecule has been a successful method to design new drug candidates in structure based drug design [25]. Thiourea and its derivatives are versatile precursor units in the synthesis of many useful heterocyclic compounds [26]. Vibrational spectroscopic studies of certain thiourea derivatives are reported in literature [27-29]. Many thiourea materials with good NLO effects have been designed and synthesized [30-35].

Pharmaceutical care products (PCCPs) are constantly polluting all types of water resources [36-38]. They are based on very stable biologically active molecules and their removal from the water is neither efficient nor economic with conventional water purification methods. A fine alternative is seen in the advanced oxidation processes which induce the degradation of the stable molecules [39-41]. Forced degradation experiments are being conducted in order to detect intermediates and investigate their toxicities towards various aquatic organisms. However, forced degradation experiments are expensive and tedious tasks. Fortunately, there are clear correlations between degradation properties and quantities that are readily calculated by DFT and MD approaches and this allows efficient rationalization and optimization of experiments related to drug stability [42].

In this work, beside investigation of fundamental reactive properties, we have also calculated BDE values in order to initially assess the degradation possibilities by autoxidation. BDEs of the remaining single acyclic bonds have also been used in order to detect the weakest bonds and therefore molecule sites where the process of degradation could start. In the same time we have determined the atoms with significant interactions with water molecules by calculations of RDFs after MD simulations.

## 2. Experimental and computational details

### 2.1. The preparation of 1-(3-bromophenyl)-3-[3-(trifluoromethyl)phenyl]thiourea

A solution of starting 3-(trifluoromethyl)aniline (0.0031 mol, 0.50 g) in anhydrous acetonitrile (10 mL) was treated with 3-bromophenylisothiocyanate (0.0031 mol) and the mixture was stirred at room temperature for 12 h. Then solvent was removed on rotary evaporator. The residue was re-crystallized from acetonitrile and then purified by column chromatography (chloroform: methanol; 9.5:0.5 vol.).

The IR spectrum was obtained on Perkin Elmer Spectrum 1000 spectrometer in KBr pellets. FT-Raman spectrum was obtained on a Nicolet 6700 FT-IR Spectrometer with NXR Ft-Raman Module, solid sample, Ge detector, excitation wavelength: 1064 nm, power at sample: maximum 150 mW, resolution:  $2.0\text{ cm}^{-1}$ , number of scans: 1064. NMR spectra ( $^1\text{H}$  and  $^{13}\text{C}$ ) for the compound were recorded on a 500MHz NMR Spectrometer (Bruker advance, Reinstetten, Germany) using deuteriated DMSO and methanol as the solvent. The chemical shift values (ppm) and coupling constants (J) are given in  $\delta$  and Hz respectively.

Yield 72%, white powder, m.p. 99-101 °C.  $^1\text{H}$  NMR (300 MHz, DMSO)  $\delta$ : 10.34 (s, 1H, NH), 10.31 (s, 1H, NH), 7.97 (s, 1H), 7.83 (m, 1H), 7.77 (d, 1H,  $J = 8.1\text{ Hz}$ ), 7.57 (t,  $J = 7.95\text{ Hz}$ , 1H), 7.52-7.43 (m, 2H), 7.37-7.28 (m, 2H).  $^{13}\text{C}$  NMR (75.4 MHz, DMSO)  $\delta$ : 180.36 (C=S), 141.06, 140.42, 130.87, 130.26, 130.02, 129.44 (q,  $J = 31.8\text{ Hz}$ ), 127.98, 127.82, 126.56, 143.09, 124.65 (q,  $J = 270.0\text{ Hz}$ ), 121.38, 120.48. HRMS (ESI) calc. for  $\text{C}_{14}\text{H}_9\text{BrF}_3\text{N}_2\text{S}$   $[\text{M} - \text{H}]^-$ : 372.9622, found: 372.9620.

### 2.2. Computational details

We have conducted detailed conformational analysis in order to obtain the lowest energy geometry of the ANF-22 molecule, which was further used for detailed investigation of

spectroscopic and reactive properties. Firstly, conformational analysis was conducted employing the MacroModel program [43], which yielded total of 98 structures. All of these structures have been geometrically optimized with Jaguar 9.0 program [44] at B3LYP/6-31G(d) level of theory to obtain the low energy conformations. Five of them with the lowest energies have been chosen and further they have been subjected to geometrical optimizations and frequency calculations at B3LYP/6-31G(d,p) level of theory, with increased integral accuracy and finer grid density. Frequency calculations yielded only positive frequencies, which assures that true ground states were located. Further, the lowest energy conformation of these five low energy conformations has been chosen for detailed calculations.

For the lowest energy conformation Jaguar program was used for calculations of average local ionization energy (ALIE), Fukui functions and bond dissociation energies (BDE) with B3LYP exchange-correlation functional [45-49] and 6-311G++(d,p), 6-31+G(d) and 6-311G(d,p) basis sets, respectively. Full linear response approach of time dependent density functional theory (TD-DFT) has been used with CAM-B3LYP [50] exchange-correlation functional and 6-31+G(d,p) basis sets. Desmond [46] program was employed for the MD simulations with OPLS 2005 force field [51] and within NPT ensemble class. Simulation time was set to 10 ns, while simple point charge (SPC) model [52] was used for the treatment of solvent. MacroModel, Jaguar and Desmond programs were used as implemented in Schrödinger Materials Science Suite 2015-4. The NLO analysis, NBO analysis, frontier molecular orbital analysis and MEP are done with the help of Gaussian software [53, 54] and Gaussview software [55]. The GAR2PED software [56] is adapted to read the outputs from the program Jaguar and the Potential energy distribution is calculated for the normal modes of vibrations of the title compound. A scaling factor value 0.9613 is applied for the theoretically obtained wave number to get better agreement with the experimental wave numbers. Charge transfer analysis has been done with Multiwfn program [57-60]. Electron density variation and  $C_{+/-}$  functions have been visualized with VMD program [61-67], while Tachyon [68] ray tracing library, as implemented in VMD, was used for rendering of figures.

### 3. Results and discussion

In the following discussion, the phenyl rings, C11-C12-C13-C14-C15-C16 and C1-C2-C3-C4-C5-C6 are designated as PhI and PhII, respectively.



literature [29]. For the title compound, the C-S bond length  $1.6764\text{\AA}$  and this lies between the values of C-S single and double bonds and the reported value is  $1.6636\text{\AA}$  [29].

At  $C_{15}$  position of the title compound, the bond angles,  $C_{14}-C_{15}-C_{16} = 122.3^\circ$ ,  $C_{14}-C_{15}-Br_{17} = 119.1^\circ$  and  $C_{16}-C_{15}-Br_{17} = 118.5^\circ$  and the asymmetry in angles is due to the presence of electronegative bromine atom. Around  $C_2$  and  $C_{11}$  positions, the angles are,  $C_1-C_2-C_3 = 119.7^\circ$ ,  $C_1-C_2-N_7 = 123.5^\circ$ ,  $C_3-C_2-N_7 = 116.7^\circ$  and  $C_{12}-C_{11}-C_{16} = 119.7^\circ$ ,  $C_{12}-C_{11}-N_9 = 118.6^\circ$ ,  $C_{16}-C_{11}-N_9 = 121.7^\circ$  which shows the interaction between the phenyl rings and thiourea moiety. The interaction between the C-S group and N-H groups are revealed by the values of the angles around  $C_8$  and the angles are,  $N_7-C_8-N_9 = 114.1^\circ$ ,  $N_7-C_8-S_{10} = 127.0^\circ$  and  $N_9-C_8-S_{10} = 118.9^\circ$ . Similarly the substitution of  $CF_3$  group changes the angles around  $C_4$  position which are  $C_3-C_4-C_5 = 120.5^\circ$ ,  $C_3-C_4-C_{18} = 119.6^\circ$  and  $C_5-C_4-C_{18} = 119.8^\circ$ . The thiourea moiety is tilted from the phenyl rings as is evident from the torsion angles,  $C_3-C_2-N_7-C_8 = 151.3^\circ$ ,  $C_1-C_2-N_7-C_8 = -31.9^\circ$ ,  $C_{16}-C_{11}-N_9-C_8 = -43.8^\circ$  and  $C_{12}-C_{11}-N_9-C_8 = 139.3^\circ$ .

### 3.2 IR and Raman spectra

Tables S2 and S3 of the supplementary materials contain the calculated scaled wave numbers, IR and Raman data of the two lowest energy conformation (ANF-22\_17 and ANF-22\_8) respectively. Experimentally obtained IR and FT-Raman spectra have been provided in Figure 2. Computationally obtained IR spectra (Figure S4 of the supplementary materials), for comparison with experimentally obtained results, has been obtained by averaging IR spectra of the two lowest energy conformers and weighting respective spectra according to their total energies.

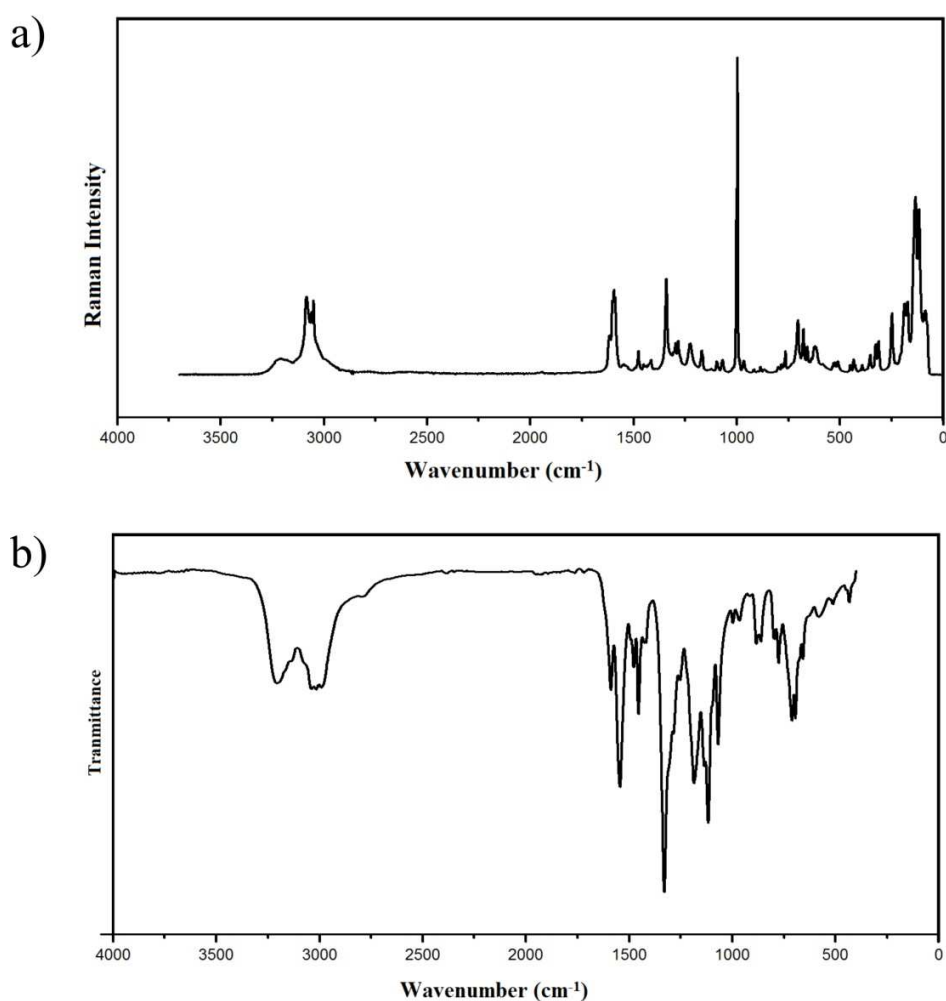


**Figure 2.** a) FT-Raman and b) FT-IR spectra of ANF-22

According to literature the NH stretching and deformation modes are expected in the regions 3330-3450 cm<sup>-1</sup> and 1400-1500, 450-600 cm<sup>-1</sup> [73] and for the title compound, the NH stretching modes are observed at 3219 cm<sup>-1</sup> in the Raman and at 3479, 3429 cm<sup>-1</sup> theoretically. The deformation modes of the NH groups are observed at 1477, 512 cm<sup>-1</sup> in the IR spectrum, 1531, 530, 511 cm<sup>-1</sup> in the Raman spectrum, while theoretically these modes were located at 1529, 1479, 531, 509 cm<sup>-1</sup>. In the present case the band at 730 cm<sup>-1</sup> in the IR spectrum and 725 cm<sup>-1</sup> in the theoretically obtained spectrum is assigned as the C=S stretching mode [73-75], which is in agreement with literature [29,76]. The band at 650 cm<sup>-1</sup> in the IR spectrum, 646 cm<sup>-1</sup> in the Raman spectrum and at 646 cm<sup>-1</sup> in the theoretically obtained IR spectrum is assigned as C-Br stretching mode of the title compound [73, 75], which is in agreement with reported values

[77,78]. According to literature, the  $\text{CF}_3$  stretching modes are expected in the regions, 1300-1100  $\text{cm}^{-1}$  and in-plane and out-of-plane bending modes in the regions, 720-440, 470-260  $\text{cm}^{-1}$  [73]. In the present case, the bands at 1140  $\text{cm}^{-1}$  in the IR spectrum, 1170, 1128  $\text{cm}^{-1}$  in the Raman spectrum and at 1170, 1145, 1055  $\text{cm}^{-1}$  in the theoretical spectrum are assigned as the  $\text{CF}_3$  stretching modes, which is in agreement with reported values [47].

For the title compound, the  $\text{CF}_3$  deformation modes are assigned at 552, 398, 313  $\text{cm}^{-1}$  in the Raman spectrum and at 530, 511, 430, 297  $\text{cm}^{-1}$  theoretically, which are in agreement with the reported values [72, 80]. For the title compound, the C-N stretching modes are assigned at 1190  $\text{cm}^{-1}$  in the IR spectrum, 1304, 1228  $\text{cm}^{-1}$  in the Raman spectrum and 1304, 1229, 1195 and 1145  $\text{cm}^{-1}$  theoretically, which agrees well with literature data [29].

For the title compound, the CH stretching modes of the phenyl rings are observed at 3040  $\text{cm}^{-1}$  in the IR spectrum, 3085  $\text{cm}^{-1}$  in the Raman spectrum for PhI and at 3133, 3066  $\text{cm}^{-1}$  in the IR spectrum, 3062, 3049  $\text{cm}^{-1}$  in the Raman spectrum for PhII. According to DFT calculations these modes are located in the range between 3073 and 3104  $\text{cm}^{-1}$ .

The ring breathing mode of the 1,3-disubstituted phenyl ring of the title compound is observed at 983  $\text{cm}^{-1}$  in the Raman spectrum and at 973 theoretically, which is expected near 1000  $\text{cm}^{-1}$  according to literature [73, 81], while the and the reported value of the ring breathing mode is 1012  $\text{cm}^{-1}$  [82].

### 3.3 NMR spectra

The absolute isotropic chemical shielding was calculated by B3LYP/GIAO model [83] and numerical values of chemical shift  $\delta_{\text{calc}} = \sigma_{\text{calc}}(\text{TMS}) - \sigma_{\text{calc}}$  together with calculated values of  $\sigma_{\text{calc}}(\text{TMS})$ , are given in Table S4.

The protons of the phenyl rings I and II resonate in the ranges, 7.09-7.78 ppm and 7.03-9.11 ppm theoretically while the experimental values are, 7.32-7.83 and 7.47-7.97 ppm. The hydrogen atoms of amide groups in this compound appear at a higher chemical shift of 10.34, 10.31 ppm experimentally while  $\delta_{\text{calc}}$  of the NH protons strongly deviate from the experimental data due to the high polarity of these bonds with values 7.25 and 7.00 ppm. For aromatic carbon atoms, the range of  $^{13}\text{C}$  NMR shifts are normally greater than 100 ppm [84, 85] and for the title compound,  $^{13}\text{C}$  NMR chemical shifts of the entire phenyl carbon atoms are greater than 100 ppm

as expected in literature. The predicted shifts lie in the ranges 120.75-144.49 ppm for PhI ring and 118.43-138.68 ppm for PhII ring, while the experimental shifts are respectively, 126.56-143.09 and 120.48-140.42 ppm. The chemical shifts of carbon atoms C8 and C18 are 177.12, 133.54 (predicted) and 180.36, 124.65 (experimentally) ppm. High chemical shift in the case of carbon atom C8 is due to the neighboring nitrogen and sulfur atoms.

### 3.1. UV spectra and charge transfer based on TD-DFT calculations

TD-DFT calculations have been done in order to predict UV spectra and the obtained results were compared with the experimentally obtained UV spectra. Also, the approach based on natural transition orbitals (NTO) [86] was used in order to investigate the topology of the most important excitations that principally dictate light absorption properties. Figure S3 of the supplementary materials contains comparison of theoretically and experimentally obtained UV spectra.

Theoretically and experimentally obtained UV spectra are in good agreement and both indicate two absorption peaks. Difference of wavelength between theoretically and experimentally obtained UV spectra is 3 or 4 nm, which is very good agreement. The only significant difference can be concluded for the absorbance of the peak located at 260 nm, but it is important that predicted UV spectra also shows that the peak located at ~200 nm is higher than the peak located at ~260 nm.

Further, electronic transitions have been checked. As in many cases, due to the size of ANF-22 molecule, TD-DFT calculations gave extensive list of orbital transitions. This makes identification of the most important electronic excitations practically impossible. However, by application of the natural transition orbitals (NTO) [86] approach this task was made possible. As opposed to the ordinary orbitals, NTOs consists of one (sometimes two or more) pair of orbitals. In the case of NTO concept, transition occurring from excited particle (occupied) to the empty hole (unoccupied) orbital [86]. The most important information (excitation energies, wavelength and oscillator strengths) on the first 20 excitations are summarized in Table 1, while in Figure 3 we have provided visualization of the frontier molecular orbitals and hole-particle orbitals of the second and ninth excitations.

Table 1. Information about the first 20 excitations of the ANF-22 compound

Excitation #	Excitation energy [eV]	Wavelength [nm]	Oscillator strength
1	4.11	301.44	0.0038
2	4.70	263.95	0.5280
3	4.75	260.81	0.2456
4	5.03	246.36	0.0322
5	5.06	245.03	0.0424
6	5.59	221.97	0.0007
7	5.82	213.00	0.0435
8	5.93	209.09	0.0652
9	6.03	205.67	0.2707
10	6.07	204.37	0.0281
11	6.14	201.88	0.0423
12	6.16	201.26	0.0516
13	6.22	199.21	0.1248
14	6.27	197.82	0.0167
15	6.33	195.91	0.0271
16	6.35	195.30	0.0414
17	6.38	194.42	0.0107
18	6.43	192.74	0.0809
19	6.44	192.61	0.1328
20	6.48	191.32	0.0726

The lowest energy excitation occurs for the energy of 4.11 eV and corresponds to the wavelength of 301 nm. According to the oscillator strength two the most important excitations are the second and the ninth excitation, with corresponding oscillator strengths of 0.5280 and 0.2707, respectively. It is interesting that both of these two most important excitations are located at wavelengths that almost completely match the experimentally measured absorption peaks. Namely, second excitation is located at the wavelength of 264 nm which is matching with experimentally measured absorption peak, while the ninth excitation is located at the wavelength of 206 nm, which is very close to the experimentally measured value of 204 nm. In Figure 3 NTOs of the frontier molecular orbitals and two the most important excitations have been provided.

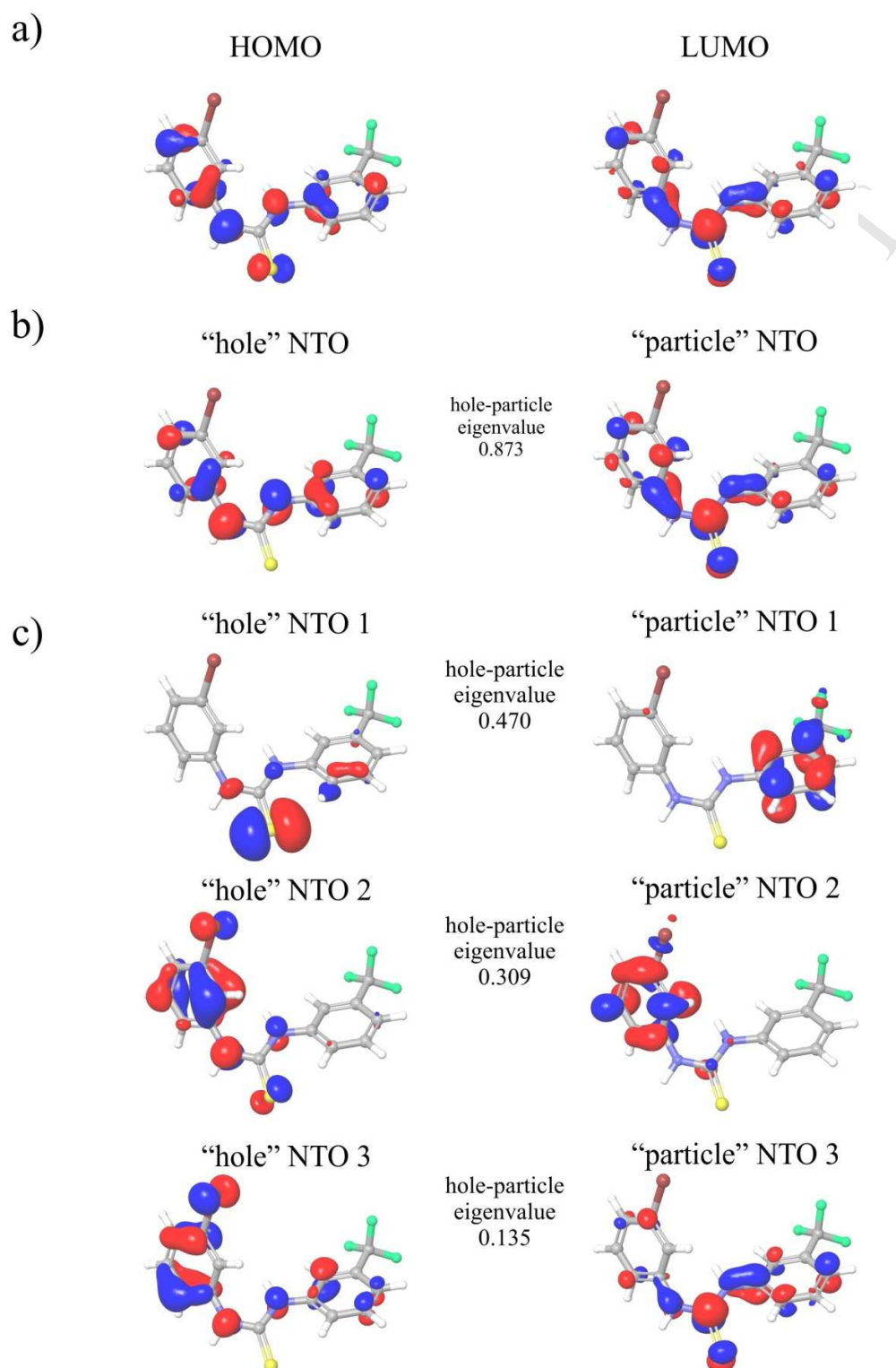


**Figure 3.** a) HOMO and LUMO orbitals and hole/particle NTOs of the b) second and c) ninth excitation

The topology of orbitals presented in Figure 3 indicates that NTOs of the second excitation match very well with the frontier molecular orbitals, indicating the importance of this excitation for the light absorption. This is also reflected with the highest value of oscillator strength in the case of the second excitation. It can also be seen in Figure 3a that HOMO and LUMO are located at the sulfur atom, “hole” NTO of the second excitation is not located at sulfur atom, while “particle” NTO of the second excitation is located at the sulfur atom. When it comes to the light absorption, the importance of sulfur atom is reflected by the fact that “hole” NTO of the first pair of the ninth excitation is clearly located at sulfur atom.

Charge transfer analysis for the lowest energy excitation based on the electron density difference has been performed by the Multiwfn program [57-60]. The method explained in reference [87], as generalized in three dimensions by creators of Multiwfn program, has been employed. According to the work [87] quantification of charge transfer can be described by the quantity known as charge transfer length (CT length). CT length is actually a distance between barycenters of  $C_+$  and  $C_-$  functions, while details on  $C_+$  and  $C_-$  functions can be checked in [87]. In this work barycenters of the  $C_+$  and  $C_-$  functions have been calculated with Multiwfn program and visualized with VMD program. In Figure 4a electron density variation as a consequence of the first excitation has been visualized with VMD program, using the isosurface value of 0.0015.

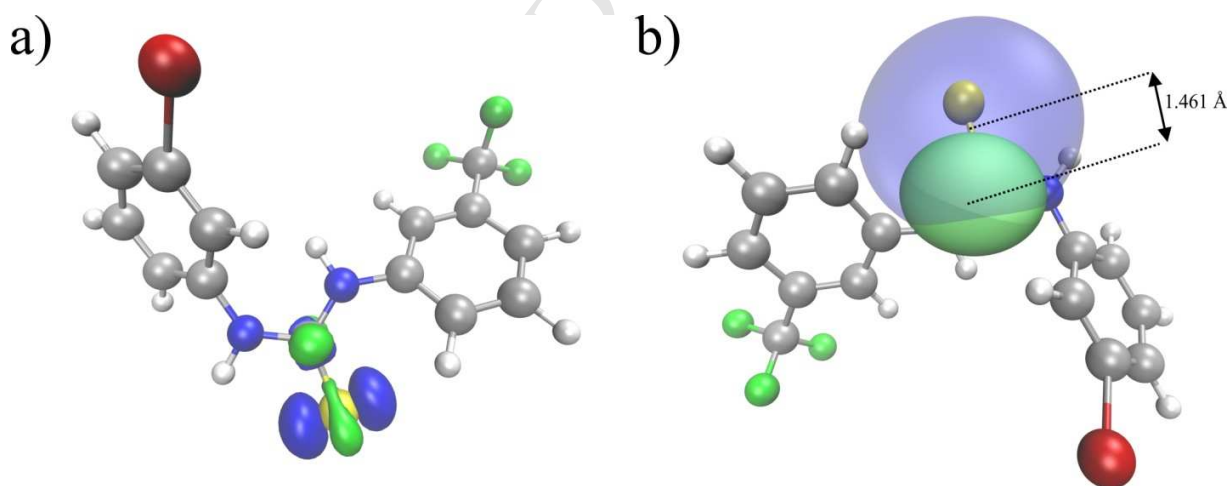


**Figure 4.** a) Electron density variation from ground to first excited state (green and blue colored areas denote positive and negative regions, respectively) of ANF-22 and b) barycenters of  $C_+$  (green) and  $C_-$  (blue) functions for ANF-22

In Figure 4a an increase of electron density is marked with green color, while blue color denotes decrease of electron density as a consequence of the lowest energy excitation. It can be seen in Figure 4a that electron density variation after the first excitation is localized in relatively small molecule area containing sulfur atom, indicating that CT length could be low and that the aforementioned excitation is of locally excited (LE) type. However, the final judgment on this will be drawn after calculation of two more important parameters. In Figure 4b we will refer to the visualization of barycenters of positive and negative parts of  $C_+$  and  $C_-$  functions.

Result provided in Figure 4b indicates that CT length in case of the lowest energy excitation of ANF-22 equals to 1.461 Å, which is value somewhere in between the CT and LE types of excitation. Thus, we have decided to use Multiwfn program again and calculate the  $\Delta r$  coefficient which, according to the paper [88], is useful when it comes to the identification of excitation type. As mentioned in reference [88], LE modes are characterized by  $\Delta r$  value lower than 2.0 Å and it can be also stated that the lower the  $\Delta r$  parameter is, the more likely is that the excitation is of local type (LE). A value of  $\Delta r$  parameter in the case of ANF-22 is 2.71 Å, clearly indicating a CT excitation type. Just for case, we have also performed a calculation of distance between centroids of electrons and holes, which is yet another indicator of excitation types, which turned out to have high value of 2.79 Å, finally indicating that the first excitation is of CT type.

### 3.4 Natural Bond Orbital Analysis

Results regarding the NBO analysis have been summarized in Table S5 of the supplementary materials. The strong inter molecular hyper conjugative interactions are:  $C_8-S_{10}$  from  $N_7$  of  $n_1(N_7) \rightarrow \sigma^*(C_8-S_{10})$  which increases the electron density 0.48220e that weakens the respective bonds  $C_8-S_{10}$  leading to stabilization of 67.31 kJ/mol;  $N_7-C_8$  from  $S_{10}$  of  $n_2(S_{10}) \rightarrow \sigma^*(N_7-C_8)$  which increases the electron density 0.06192e that weakens the respective bonds  $N_7-C_8$  leading to stabilization of 12.10 kJ/mol;  $C_8-S_{10}$  from  $N_9$  of  $n_1(N_9) \rightarrow \sigma^*(C_8-S_{10})$  which increases the electron density 0.48220e that weakens the respective bonds  $C_8-S_{10}$  leading to stabilization of 67.62 kJ/mol;  $C_{18}-F_{20}$  from  $F_{19}$  of  $n_3(F_{19}) \rightarrow \sigma^*(C_{18}-F_{20})$  which increases the electron density 0.10318e that weakens the respective bonds  $C_{18}-F_{20}$  leading to stabilization of 12.73 kJ/mol;  $C_{18}-F_{20}$  from  $F_{21}$  of  $n_3(F_{21}) \rightarrow \sigma^*(C_{18}-F_{20})$  which increases the electron density 0.10318e that weakens

the respective bonds C<sub>18</sub>-F<sub>20</sub> leading to stabilization of 11.23kJ/mol; C<sub>18</sub>-F<sub>19</sub> from F<sub>20</sub> of n<sub>3</sub>(F<sub>20</sub>)→σ\*(C<sub>18</sub>-F<sub>19</sub>) which increases the electron density 0.10155e that weakens the respective bonds C<sub>18</sub>-F<sub>19</sub> leading to stabilization of 12.60 kJ/mol; C<sub>15</sub>-C<sub>14</sub> from Br<sub>17</sub> of n<sub>3</sub>(Br<sub>17</sub>)→π\*(C<sub>15</sub>-C<sub>14</sub>) which increases the electron density 0.38276e that weakens the respective bonds C<sub>15</sub>-C<sub>14</sub> leading to stabilization of 9.88kJ/mol. The orbital with low occupation number are high energies are: n<sub>2</sub>(F<sub>19</sub>), n<sub>2</sub>(F<sub>21</sub>), n<sub>3</sub>(F<sub>20</sub>) with energies, -0.42241, -0.41665, -0.42228a.u and considerable p-characters, 100, 99.82, 99.98% and low occupation numbers, 1.94864, 1.94826, 1.93155 while the orbital with high occupation numbers and low energies are: n<sub>1</sub>(F<sub>19</sub>), n<sub>1</sub>(F<sub>21</sub>), n<sub>2</sub>(F<sub>20</sub>) with energies, -1.05684, -1.05749, -0.42300a.u. and p-characters, 29.19, 28.40, 100% and occupation numbers, 1.98707, 1.98755, 1.94924. Thus, a very close to pure p-type lone pair orbital participates in the electron donation to the σ\*(C<sub>8</sub>-S<sub>10</sub>) orbital for n<sub>1</sub>(N<sub>7</sub>)→σ\*(C<sub>8</sub>-S<sub>10</sub>), σ\*(N<sub>7</sub>-C<sub>8</sub>) orbital for n<sub>2</sub>(S<sub>10</sub>)→σ\*(N<sub>7</sub>-C<sub>8</sub>), σ\*(C<sub>8</sub>-S<sub>10</sub>) orbital for n<sub>1</sub>(N<sub>9</sub>)→σ\*(C<sub>8</sub>-S<sub>10</sub>), σ\*(C<sub>18</sub>-F<sub>20</sub>) orbital for n<sub>3</sub>(F<sub>19</sub>)→σ\*(C<sub>18</sub>-F<sub>20</sub>), σ\*(C<sub>18</sub>-F<sub>20</sub>) orbital for n<sub>3</sub>(F<sub>21</sub>)→σ\*(C<sub>18</sub>-F<sub>20</sub>), σ\*(C<sub>18</sub>-F<sub>19</sub>) orbital for n<sub>3</sub>(F<sub>20</sub>)→σ\*(C<sub>18</sub>-F<sub>19</sub>), π\*(C<sub>15</sub>-C<sub>14</sub>) interactions in the compound.

### 3.5 Nonlinear optical properties

For the title compound, first hyperpolarizability and second hyperpolarizability are respectively,  $2.5749 \times 10^{-30}$  and  $-20.985 \times 10^{-37}$  esu and these values of the investigated molecule clearly reveal that they have nonlinear optical behavior with non-zero values. The reported value of the first hyperpolarizability of phenyl thiourea derivatives is  $1.86 \times 10^{-30}$  esu [29] and the first hyperpolarizability of the title compound is 19.81 times that of the standard NLO material urea [89]. The C-N bond lengths in the title compound are in between a single and double bond and hence there is an extended π-electron delocalization over the thiourea group [90] which is responsible for the nonlinearity of the system.

### 3.6 Frontier molecular orbital analysis

HOMO and LUMO energy values are very important parameters for quantum chemistry and HOMO is the outermost orbital, tends to give electrons and act as an electron donor while the LUMO accepts electrons [91]. The HOMO-LUMO plot of the title compound is shown in Figure S4 of the supplementary materials. According to the B3LYP/6-31G(d,p) method, the HOMO and LUMO energy values are -7.327eV and -4.574eV. The ionization energy and

electron affinity can be expressed as:  $I = -E_{\text{HOMO}} = 7.327$ ,  $A = -E_{\text{LUMO}} = 4.574\text{eV}$  [92]. The hardness  $\eta$  and chemical potential  $\mu$  are given the following relations  $\eta = (I - A)/2$  and  $\mu = -(I+A)/2$ , where  $I$  and  $A$  are the first ionization potential and electron affinity of the chemical species [93]. For the title compound, HOMO-LUMO energy gap = 2.753eV, Ionization potential,  $I = 7.327\text{eV}$ , Electron affinity  $A = 4.574\text{eV}$ , global hardness  $\eta = 1.377\text{eV}$ , chemical potential  $\mu = -5.951\text{eV}$ , global electrophilicity index =  $\mu^2/2\eta = 12.859\text{eV}$ .

### 3.7. MEP and ALIE surfaces, non-covalent interactions and Fukui functions

In order to identify sites suitable for nucleophilic reactions or electrophilic attacks, the molecular electrostatic potential map of the title compound was calculated at the B3LYP/6-31G (6D, 7F) level and given in Figure 5a.

The red and yellow color which indicates the negative regions of the molecule are electrophilic reactivity regions and blue color regions are positive which indicates the nucleophilic reactivity regions in the MEP plot [94-96]. For the title compound, the electrophilic regions are phenyl rings, CS group and nucleophilic regions are mainly NH groups.

Sites of ANF-22 molecule that are possibly prone to electrophilic attacks in this work have been determined by calculations of ALIE values. This quantity was introduced by Sjoberg et al. [97, 98] and it is defined as sum of orbital energies weighted by the orbital densities according to the following equation:

$$I(r) = \sum_i \frac{\rho_i(\vec{r}) \varepsilon_i}{\rho(\vec{r})}, \quad (1)$$

where  $\rho_i(\vec{r})$  represents the electronic density of the  $i$ -th molecular orbital at the point  $\vec{r}$ ,  $\varepsilon_i$  represents the orbital energy and  $\rho(\vec{r})$  is the total electronic density function. This descriptor indicates the amount of energy needed for the removal of electrons from certain molecule places. The lower the ALIE is, electrons are easier removed. In this work ALIE values are mapped to the electron density surface and in such way obtained surface indicate molecule sites where electrons are least tightly bound, Figure 5b.

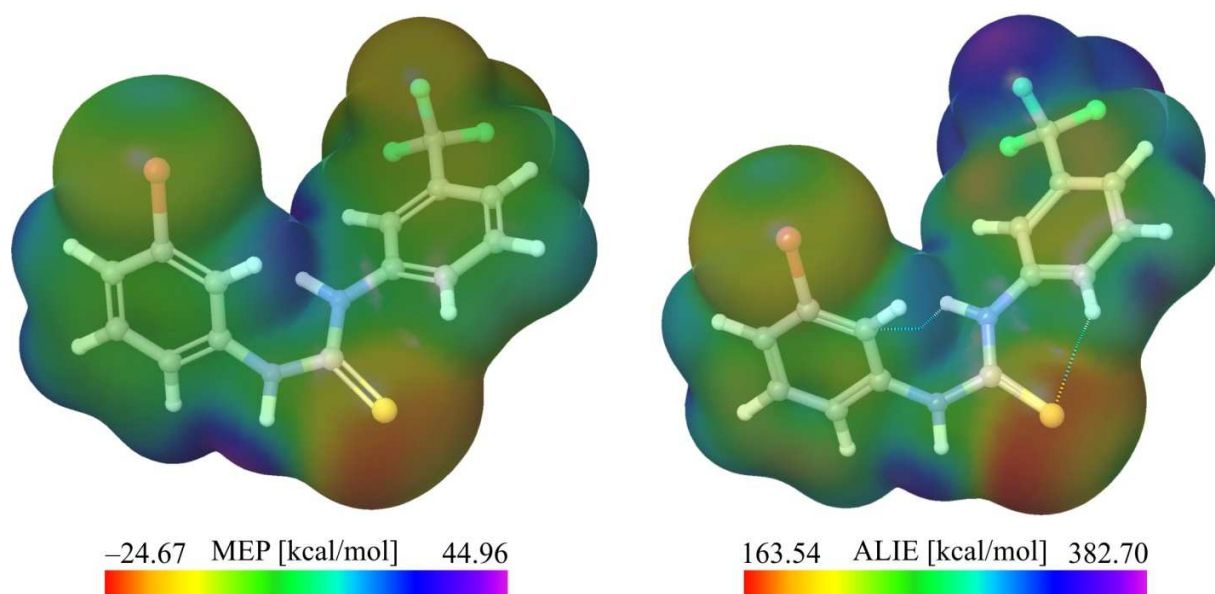


**Figure 5.** a) MEP and b) ALIE surface of the ANF-22 molecule

It can be seen in Figure 5 that sulfur atom is certainly very important reactive center from the aspect of electrophilic attacks. In order to remove the electron from the area in the near vicinity of sulfur atom it is necessary to spend around 163 kcal/mol, according to the calculated ALIE descriptor. On the other side the highest values of ALIE descriptor are calculated in the near vicinity of fluorine atoms and these locations are molecule sites where electrons are tightly bound. In the near vicinity of fluorine atoms the ALIE values equals more than 382 kcal/mol. According to the results presented in Figure 5b, ANF-22 molecule is also characterized by formation of two intra-molecular non-covalent interactions, between atoms C16–H26 and between atoms S10–H22. Both of these non-covalent interactions have very similar strengths, 0.014 electron/bohr<sup>3</sup>.

Tracking the electron density changes as a consequence of addition or removal of charge allows one to additionally determine important reactive sites. This can be done by utilization of Fukui functions, which are in Jaguar program calculated in the finite difference approximation according to the following equations:

$$f^+ = \frac{(\rho^{N+\delta}(r) - \rho^N(r))}{\delta}, \quad (2)$$

$$f^- = \frac{(\rho^{N-\delta}(r) - \rho^N(r))}{\delta}, \quad (3)$$

where  $N$  denotes the number of electrons in the reference state of the molecule and  $\delta$  represents the fraction of electron, which is set to be 0.01 [99].

Fukui  $f^+$  and  $f^-$  functions respectively indicate how electron density changes when certain amount of charge is added or removed. Therefore, these functions practically show where electron density increases and decreases when molecule acts as electrophile and nucleophile, respectively. In this work the representation of Fukui functions has been done by mapping of their values to the electron density surface, Figure 6.

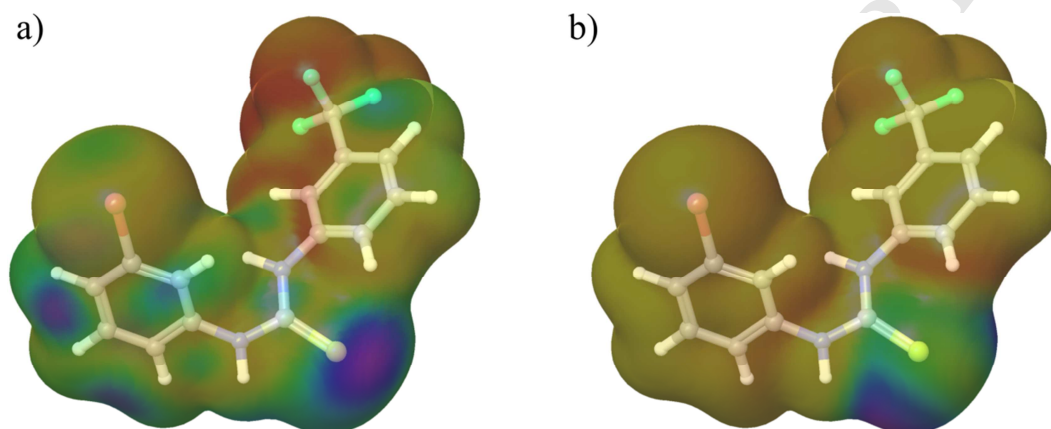


**Figure 6.** Fukui a)  $f^+$  and b)  $f^-$  function of ANF22

For the visualization of Fukui functions in Figure 6 the following color coding has been used. Namely, in the case of Fukui  $f^+$  function presented in Figure 6a, purple color indicates molecule sites where electron density increases as a consequence of charge addition. On the other side, in the case of Fukui  $f^-$  function presented in Figure 6b, red color indicates molecule sites where electron density decreases with the removal of charge. Results in Figure 6a again emphasize the reactive importance of sulfur atom. Besides sulfur atom, purple color is also located in the near vicinity of carbon atoms C12 and C14, indicating that these locations are the ones where electron density increases when ANF-22 molecule acts as an electrophile. On the other side, yellow to red color is delocalized practically over the whole molecule, indicating the decrease in the charge density when molecule acts as a nucleophile, except in the near vicinity of sulfur atom and carbon atom C8.

### 3.8 Degradation and reactive properties based on the autoxidation and hydrolysis

As more and more pharmaceutical molecules are entering the water streams due to the overuse and improper handling, beside synthesis of new molecules it is also necessary to understand how they can be efficiently removed from the water [100,101].

Because strong correlation exists between degradation by autoxidation and BDEs, DFT calculations are very useful for the overall understanding of degradation properties of drugs [100-102]. On the other side understanding the interactions of drug molecules with water is also of great importance. In this case MD simulations can be particularly useful for the determination of molecule's atoms with pronounced interaction with water molecules, which can be useful for the understanding of hydrolysis.

Concerning the degradation by autoxidation it is useful to emphasize that this mechanism is closely related to the possibility for hydrogen atoms to be abstracted. If the BDE for hydrogen abstraction has the proper value, than that molecule location can be considered as probably suitable for the start of autoxidation process. It is also crucial to determine the proper interval of BDE values suitable for the C-H dissociation. From one side it is well known that all peroxy radicals have BDE in the range of 87–92 kcal/mol [101,103]. On the other side the study of Wright et al. [102] shows that BDE values in the interval between 75 to 85 kcal/mol indicate that molecule is highly prone to the autoxidation. Also, Gryn'ova et al. [104] stated that thermodynamic favorability of C–H bond dissociation probability is strongly favored for BDE values lower than 85 kcal/mol, disfavored for BDE values higher than 90 kcal/mol and questionable for BDE values between 85 to 90 kcal/mol. BDE values calculated for all single acyclic bonds are presented in Figure 7.

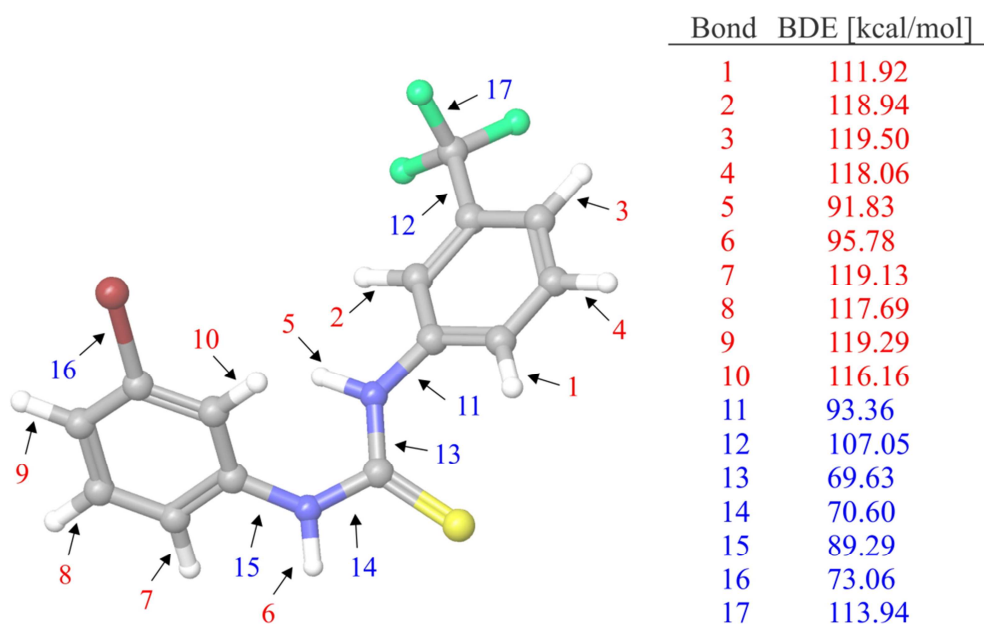


**Figure 7.** BDE for hydrogen abstraction in case of ANF-22 molecule

Results presented in Figure 7 clearly indicate the high stability of the ANF-22 molecule. The lowest BDE value for the hydrogen abstraction is almost 92 kcal/mol. This indicates that the mentioned molecule is highly stable in the open air and in the presence of oxygen. BDE values for the remaining single acyclic bonds served us also to determine the weakest bonds and therefore the locations where the process of degradation could start. Thanks to the results in Figure 7, it can be concluded that the weakest bonds are the ones denoted with numbers 13 and 14. BDE values in these two cases are around 70 kcal/mol and they clearly emphasize the importance of sulfur atom, which is in their close vicinity.

In order to locate the atoms of ANF-22 molecule with relatively pronounced interactions with water molecules we have calculated RDFs after MD simulations. RDF,  $g(r)$ , is the probability of finding a particle in the distance  $r$  from another particle [105]. RDFs of atoms with significant interactions with water molecules are presented in Figure 8.

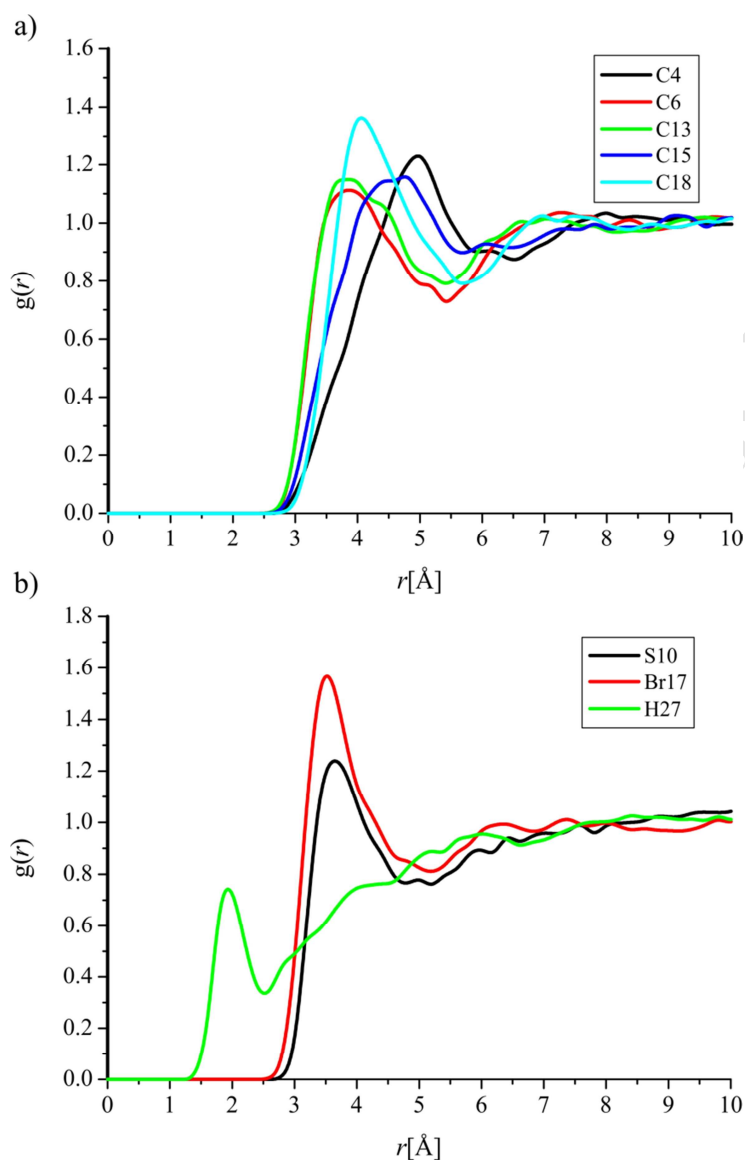


**Figure 8.** RDFs of molecule ANF-22

According to the profiles of RDFs in Figure 8 it can be seen that total of eight atoms have significant interactions with water molecules. Five of them are carbon atoms while the remaining ones are one sulfur, bromine and hydrogen atoms. Carbon atom with the highest  $g(r)$  values is atom C18, with corresponding  $g(r)$  value of almost 1.4. On the other side carbon atoms C6 and C13 have the shortest peak distances, located at around 3.5 Å. The most important RDF is calculated for hydrogen atom H27, which has the peak distance lower than 2 Å. Bromine and sulfur atoms have much higher maximal  $g(r)$  values, but their peak distances are located at

around 3.5 Å. The fact that sulfur atom and hydrogen atom H27 have very pronounced interactions with water could be very important because both of these two atoms are located in the near vicinity of the bond which is the weakest according to the BDE values, meaning that the hydrolysis could be of importance.

### 3.10 Molecular docking

The decahydroisoquinoline scaffold bearing a phenyl tetrazole is a GluK1 antagonist with potential as oral analgesics [106]. The aryl thiourea derivatives show antitumor, antimicrobial and analgesic activity [107]. Thiourea derivatives exhibit their analgesic activity in mice (*Mus musculus*), and showed a better analgesic activity compared to Na-diclofenac [108]. High resolution crystal structure of decahydroisoquinoline antagonist was obtained from the RSCB protein data bank website with PDB ID: 4MF3. Using Auto Dock-Vina software [109] all molecular docking calculations were performed. All the docking protocol was prepared as reported in literature [110]. In Figure S5 of the supplementary materials, surface view of the docked ligand embedded in the catalytic site of decahydroisoquinoline antagonist has been visualized, while weak non-covalent interactions between the active site of the substrate and the ligand have been visualized in Figure S6 of the supplementary materials. Besides visualization of the docked ligand in Table 2 we are providing information about the binding affinities.

Table 2. The binding affinity values of the title compound to decahydroisoquinoline antagonist

Mode	Affinity (kcal/mol)	Distance from best mode (Å)	
		RMSD l.b.	RMSD u.b.
1	-7.1	0.000	0.000
2	-6.9	6.513	8.313
3	-6.8	9.875	12.403
4	-6.8	5.823	8.679
5	-6.6	1.733	2.403
6	-6.6	8.656	11.089
7	-6.6	9.594	11.757
8	-6.6	11.973	13.842
9	-6.5	9.032	11.836

Amino acids Glu15, Ser194 form halogen interactions with CF<sub>3</sub>. Glu14 shows  $\pi$ -anion interaction with phenyl ring and NH group and Tyr197 exhibit  $\pi$ -alkyl interaction with CF<sub>3</sub>.

Thanks to the indicated weak non-covalent interactions it can be concluded that the docked ligand forms a stable complex with decahydroisoquinoline antagonist with the highest binding affinity value of  $-7.1$  kcal/mol. These results indicate that title compound could be considered as a lead compound for the development of new analgesic drug.

#### 4. Conclusion

The detailed interpretation of the vibrational spectra of 1-(3-bromophenyl)-3-[3-(trifluoromethyl)phenyl]thiourea have been carried out with the help of potential energy distribution. Excellent agreement for the calculated vibrational wave numbers with the experiment whenever available has been found. Detailed analysis of NBO, NMR, frontier molecular orbital analysis and MEP are reported. Thanks to the ALIE values sulfur atom is recognized to be possibly prone to electrophilic attacks. The importance of sulfur atom was confirmed by Fukui functions as well, which also recognized carbon atoms C14 and C16 as important reactive centers. Two intramolecular noncovalent interactions have been detected, with very similar strengths. From the aspect of TD-DFT calculations, the most important excitations have been identified while NTOs indicated the most important molecule areas for the light absorption. Detailed charge transfer analysis indicated that the first excitation is of CT type. The lowest BDE values for abstraction of hydrogen atoms are higher than 90 kcal/mol and it is hard to expect that this molecule is sensitive towards autoxidation. Sulfur atom and hydrogen atom H27 have pronounced interactions with water molecules, which could be meaningful since these two atoms are in the close vicinity of the bonds that are the weakest according to the BDEs. The docked title compound forms a stable complex with decahydroisoquinoline antagonist with a binding affinity value of  $-7.1$  kcal/mol and can be a lead compound for developing new analgesic drug.

#### Acknowledgments

Part of this work has been performed thanks to the support received from Schrödinger Inc. Part of this study was conducted within the projects supported by the Ministry of Education, Science and Technological Development of Serbia, grant numbers ON171039, TR34019.

**References**

- [1] A. Bielenica, J. Stefańska, K. Stępień, A. Napiórkowska, E. Augustynowicz-Kopeć, G. Sanna, S. Madeddu, S. Boi, G. Giliberti, M. Wrzosek, M. Struga, Synthesis, cytotoxicity and antimicrobial activity of thiourea derivatives incorporating 3-(trifluoromethyl)phenyl moiety, *Eur. J. Med. Chem.* 101 (2015) 111-125.
- [2] S. Saeed, N. Rashid, P.G. Jones, M. Ali, R. Hussain, Synthesis, characterization and biological evaluation of some thiourea derivatives bearing benzothiazole moiety as potential antimicrobial and anticancer agents, *Eur. J. Med. Chem.* 45 (2010) 1323–1331.
- [3] R.M. Kumbhare, T. Dadmal, U. Kosurkar, V. Sridhar, J.V. Rao, Synthesis and cytotoxic evaluation of thiourea and N-bis-benzothiazole derivatives, a novel class of cytotoxic agents, *Bioorg. Med. Chem. Lett.* 22 (2012) 453–455.
- [4] A. Bielenica, K. Stępień, A. Napiórkowska, E. Augustynowicz-Kopeć, S. Krukowski, M. Włodarczyk, M. Struga, Synthesis and antimicrobial activity of 4-chloro-3-nitrophenylthiourea derivatives targeting bacterial type II topoisomerases, *Chem. Biol. Drug Des.* 87(2016) 905-917.
- [5] J. Stefanska, D. Szulczyk, A.E. Koziol, B. Mirosław, E. Kedzierska, S. Fidecka, B. Busonera, G. Sanna, G. Giliberti, P. La Colla, M. Struga, Disubstituted thiourea derivatives and their activity on CNS, synthesis and biological evaluation, *Eur. J. Med. Chem.* 55 (2012) 205-213.
- [6] O.J. D'Cruz, S. Qazi, S. Yiv, F.M. Uckun, A novel vaginal microbicide containing the rationally designed anti-HIV compound HI-443 (N'-[2-(2-thiophene)ethyl]-N'-[2-(5-bromopyridyl)]thiourea), *Expert. Opin. Investig. Drugs.* 21 (2012) 265–279.
- [7] S. Karakuş, S. Güniz Küçükgülzel, I. Küçükgülzel, E. De Clercq, C. Pannecouque, G. Andrei, R. Snoeck, F. Sahin, O.F. Bayrak, Synthesis, antiviral and anticancer activity of some novel thioureas derived from N-(4-nitro-2-phenoxyphenyl)-methanesulfonamide, *Eur. J. Med. Chem.* 44 (2009) 3591–3595.
- [8] J.D. Bloom, R.G. Dushin, K.J. Curran, F. Donahue, E.B. Norton, E. Terefenko, T.R. Jones, A.A. Ross, B. Feld, S.A. Lang, M.J. DiGrandi, Thiourea inhibitors of herpes viruses. Part 2. N-benzyl-N-arylthiourea inhibitors of CMV, *Bioorg. Med. Chem. Lett.* 14 (2004) 3401–3406.

- [9] M. Struga, J. Kossakowski, E. Kedzierska, S. Fidecka, J. Stefańska, Synthesis and pharmacological activity of urea and thiourea derivatives of 4-azatricyclo[5.2.2.0(2,6)]undec-8-ene-3,5-dione, *Chem. Pharm. Bull. (Tokyo)*, 55 (2007) 796-799.
- [10] A. Bielenica, E. Kedzierska, S. Fidecka, H. Maluszynska, B. Mirosław, A.E. Koziol, J. Stefanska, S. Madeddu, G. Giliberti, G. Sanna, M. Struga, Synthesis, antimicrobial and pharmacological evaluation of thiourea derivatives of 4H-1,2,4-triazole, *Lett. Drug Des. Discov.* 12 (2015) 263-276.
- [11] A. Bielenica, E. Kędzierska, M. Koliński, S. Kmiecik, A. Koliński, F. Fiorino, B. Severino, E. Magli, A. Corvino, I. Rossi, P. Massarelli, A.E. Koziol, A. Sawczenko, M. Struga, 5-HT<sub>2</sub> receptor affinity, docking studies and pharmacological evaluation of a series of 1,3-disubstituted thiourea derivatives, *Eur. J. Med. Chem.* 116 (2016) 173-186.
- [12] M. Struga, J. Kossakowski, A.E. Koziol, T. Lis, E. Kędzierska, S. Fidecka, Synthesis and pharmacological activity of thiourea derivatives of 1,7,8,9-tetramethyl-4-azatricyclo[5.2.1.02.,6]dec-8-ene-3,4-dione, *Lett. Drug. Des. Discov.* 6 (2009) 445-450.
- [13] B.K. Kaymakçioğlu, S. Rollas, E. Körçeğez, F. Arıcıoğlu, Synthesis biological evaluation of new N-substituted-N-(3,5-di/1,3,5-trimethylpyrazole-4-yl)thiourea/urea derivatives, *Eur. J. Pharm. Sci.* 26 (2005) 97-103.
- [14] S. Karakus, B. Koçyiğit-Kaymakçioğlu, H.Z. Toklu, F. Arıcıoğlu, S. Rollas, Synthesis and anticonvulsant activity of new N-(Alkyl/substituted aryl)-N'-[4-(5-cyclohexylamino)1,3,4-thiadiazole-2-yl]phenyl]thioureas, *Arch. Pharm. (Weinheim)*. 342 (2009) 48-53.
- [15] M. Struga, S. Rosolowski, J. Kossakowski, J. Stefanska, Synthesis and microbiological activity of thiourea derivatives of 4-azatricyclo[5.2.2.0(2,6)]undec-8-ene-3,5-dione, *Arch. Pharm. Res.* 33(2010) 47-54.
- [16] S. Chen, G. Wu, H. Zeng, Preparation of high antimicrobial activity thiourea chitosan-Ag<sup>+</sup> complex, *Carbohydrate Polym.* 60 (2005) 33-38.
- [17] H. Arslan, N. Duran, G. Borekci, C. KorayOzer, C. Akbay, Antimicrobial activity of some thiourea derivatives and their nickel and copper complexes, *Molecules* 14 (2009) 519-527.

- [18] N. Dolan, D.P. Gavin, A. Eshwika, K. Kavanagh, J. McGinley, J.C. Stephens, Synthesis, antibacterial and anti-MRSA activity, in vivo toxicity and a structure activity relationship study of a quinolinethiourea, *Bioorg. Med. Chem. Lett.* 26 (2016) 630-635.
- [19] G.V. Sharma, A. Ramesh, A. Singh, G. Srikanth, V. Jayaram, D. Duscharia, J.H. Jun, R. Ummani, S.V. Mlahotra, Imidazole derivatives show anticancer potential by inducing apoptosis and cellular senescence, *Med. Chem. Comm* 5 (2014) 1751-1760.
- [20] Q. Su, S. Ioannidis, C. Chuaqui, L. Almedia, M. Alimzhanov, G. Bebemitz, K. Bell, M. Block, T. Howard, S. Huang, D. Huszar, J.A. Reed, C. Rivard Costa, J. Shi, M. Su, M. Ye, M. Zind, *J. Med. Chem.* 57 (2013) 144-158.
- [21] H.M. Alkahtani, A.Y. Abbas, S. Wang, Synthesis and biological evaluation of benzo[d]imidazole derivatives as potential anti-cancer agents, *Bioorg. Med. Chem. Lett.* 22 (2012) 1317-1321.
- [22] B. Narasimhan, D. Sharma, P. Kumar, Biological importance of imidazole nucleus in the new millenium, *Med. Chem. Res.* 20 (2011) 1119-1140.
- [23] D. Obinata, A. Ito, K. Fujiwara, K. Takavama, D. Ashikari, Y. Murata, K. Yamaguchi, T. Urano, T. Fujimura, N. Fukuda, M. Soma, T. Watanabe, H. Naqase, S. Inoue, S. Takahashi, Pyrrole imidazole polyamide targeted to break fusion sites in TMPRSS2 and ERG gene fusion represses prostate tumor growth, *Cancer Sci.* 105 (2014) 1272-1278.
- [24] Y.W. Han, T. Matsumoto, H. Yokota, G. Kashiwazaki, H. Morinaqa, T. Bando, Y. Harada, H. Sugiyama, Binding of hairpin pyrrole and imidazole polyamides to DNA: relationship between torsion angle and association rate constants, *Nucleic Acids Res.* 40 (2012) 11510-11517.
- [25] J.A. War, S.K. Srivastava, S.D. Srivastava, Synthesis and DNA binding study of imidazole linked thiazolidinone, *Luminescence* (2016) doi: 10.1002/bio.3156.
- [26] A.R. Katrizky, *Advances in Heterocyclic Chemistry*, Academic Press, New York, 1983.
- [27] W. Yang, W. Zhou, Z. Zhang, Structural and spectroscopic study of N-2-fluorobenzoyl-N-4-methoxyphenylthiourea, *J. Mol. Struct.* 828 (2007) 46-73.
- [28] H.M. Badawi, Structural stability, C-N internal rotations and vibrational spectral analysis of non-planar phenylurea and phenylthiourea, *Spectrochim. Acta* 72 (2009) 523-527.
- [29] C.Y. Panicker, H.T. Varghese, A. George, P.K.V. Thomas, FT-IR, FT-Raman and ab initio studies of 1,3-diphenyl thiourea, *Eur. J. Chem.* 1 (2010) 173-178.

- [30] N. Zhang, M.H. Jiang, D.R. Yuan, D. Xu, X.T. Tao, Z.S. Shao, The quality and performance of the organometallic complex nonlinear optical material tri-allylthiourea cadmium chloride (ATCC), *J. Cryst. Growth* 102 (1990) 581-584.
- [31] P.M. Ushasree, R. Muralidharan, R. Jayavel, P. Ramasamy, Growth of bis(thiourea) cadmium chloride single crystals – a potential NLO material of organometallic complex, *J. Cryst. Growth*, 218 (2000) 365-371.
- [32] M. Qussaid, P. Becker, C.C.Nedelec, Raman and infrared spectra of bis(thiourea)zinc chloride,  $Zn[CS(NH_2)_2]_2Cl_2$  single crystal, *Phys. Stat. Sol.(b)* 207 (1998) 499-507.
- [33] H.O. Marcy, L.F. Warren, M.S. Webb, C.A. Ebbers, S.P. Velsko, G.C. Kennedy, G.C. Catella, Second harmonic generation in zinc tris(thiourea) sulfate, *Appl. Opt.* 31 (1992) 5051-5060.
- [34] K. Selvaraju, R. Valluvan, S. Kumararaman, Growth and characterization of a new metal organic crystal, potassium thiourea iodide, *Mater. Lett.* 60 (2006) 3130-3132.
- [35] K. Selvaraju, R. Valluvan, S. Kumararaman, A new metal organic crystal, potassium thiourea chloride, *Mater.Lett.* 61 (2007) 751-753.
- [36] A. Golubović, B. Abramović, M. Šćepanović, M. Grujić-Brojčin, S. J. Armaković, I. Veljković, B. Babić, Z. Dohčević-Mitrović, Z. Popović, Improved efficiency of sol-gel synthesized mesoporous anatase nanopowders in photocatalytic degradation of metoprolol, *Mater. Res. Bull.* 48 (2013) 1363-1371.
- [37] R. Ma, B. Wang, S.Lu, Y. Zhang, L. Yin, J. Huang, S. Deng, Y. Wang, G. Yu, Characterization of pharmaceutically active compounds in Dongiting Lake, China: Occurrence, chiral profiling and environmental risk, *Sci. Total Environ.* 557 (2016) 268-275.
- [38] S.J. Armaković, S. Armaković, N.L. Finčur, F. Šibul, D. Vione, J.P. Šetrajčić, B. Abramović, Influence of electron acceptors on the kinetics of metoprolol photocatalytic degradation in  $TiO_2$  suspension: A combined experimental and theoretical study, *RSC Advances* 5 (2015) 54589-54604.
- [39] S.J. Armaković, M. Grujić-Brojčin, M. Šćepanović, S. Armaković, A. Golubović, B. Babić, and B.F. Abramović, Efficiency of La-doped  $TiO_2$  calcined at different temperatures in photocatalytic degradation of  $\beta$ -blockers. *Arab. J. Chem.* (2017) Article in Press, <https://doi.org/10.1016/j.arabjc.2017.01.001>

- [40] S. Armaković, S.J. Armaković, and B.F. Abramović, Theoretical investigation of loratadine reactivity in order to understand its degradation properties: DFT and MD study. *J. Mol. Mod.* 22 (2016) 240.
- [41] B. Sureshkumar, Y.S. Mary, C.Y. Panicker, S. Suma, S. Armaković, S.J. Armaković, C. Van Alsenoy, and B. Narayana, Quinoline derivatives as possible lead compounds for anti-malarial drugs: Spectroscopic, DFT and MD study. *Arab. J. Chem.* (2017) Article in Press, <https://doi.org/10.1016/j.arabj.2017.07.006>
- [42] P. Lienard, J. Gavartin, G. Boccardi, M. Meunier, Predicting drug substances autoxidation, *Pharm. Res.* 32 (2015) 300-310.
- [43] Schrödinger Release 2015-4: MacroModel, Schrödinger, LLC, New York, NY, 2015.
- [44] A.D. Bochevarov, E. Harder, T.F. Hughes, J.R. Greenwood, D.A. Braden, D.M. Philipp, D. Rinaldo, M.D. Halls, J. Zhang, R.A. Friesner, Jaguar: A High performance Quantum Chemistry Software Program with Strengths in Life and Materials Sciences, *Int. J. Quantum Chem.* 113 (2013) 2110-2142.
- [45] A.D. Becke, Density functional thermochemistry. III. The role of exact exchange, *J. Chem. Phys.* 98 (1993) 5648-5652.
- [46] D. Shivakumar, J. Williams, Y. Wu, W. Damm, J. Shelley, W. Sherman, Prediction of absolute solvation free energies using molecular dynamics free energy perturbation and the OPLS force field, *J. Chem. Theory Comput.* 6 (2010) 1509-1519.
- [47] Z. Guo, U. Mohanty, J. Noehre, T.K. Sawyer, W. Sherman, G. Krilov, Probing the  $\alpha$ -helical structural stability of stapled p53 peptides: Molecular dynamics simulations and analysis, *Chem. Biol. Drug Design* 75 (2010) 348-359.
- [48] K.J. Bowers, E. Chow, H. Xu, R.O. Dror, M.P. Eastwood, B.A. Gregersen, J.L. Klepeis, I. Kolossvary, M.A. Moraes, F.D. Sacerdoti, *Scalable algorithms for molecular dynamics simulations on commodity clusters.* in *SC 2006 Conference, Proceedings of the ACM/IEEE.* 2006. IEEE.
- [49] *Schrödinger Release 2015-4: Desmond Molecular Dynamics System, version 4.4, D. E. Shaw Research, New York, NY, 2015. Maestro-Desmond Interoperability Tools, version 4.4, Schrödinger, New York, NY, 2015.* 2015.

- [50] T. Yanai, D.P. Tew, N.C. Handy, A new hybrid exchange–correlation functional using the Coulomb-attenuating method (CAM-B3LYP), *Chem. Phys. Lett.* 393(2004) 51-57.
- [51] J.L. Banks, H.S. Beard, Y. Cao, A.E. Cho, W. Damm, R. Farid, A.K. Felts, T.A. Halgren, D.T. Mainz, J.R. Maple, R. Murphy, DM. Philipp, MP. Repasky, LY. Zhang, BJ. Berne, RA. Friesner, E. Gallicchio, RM. Lew, *J. Comput. Chem.* 26 (2005) 1752-1780.
- [52] H.J. Berendsen, J.P. Postma, W.F. van Gunsteren, J. Hermans, *Interaction models for water in relation to protein hydration*, in *Intermolecular forces*. 1981, Springer. p. 331-342.
- [53] Gaussian 09, Revision C.01, M.J. Frisch, G.W. Trucks, H.B. Schlegel, G.E. Scuseria, M.A. Robb, J.R. Cheeseman, G. Scalmani, V. Barone, B. Mennucci, G.A. Petersson, H. Nakatsuji, M. Caricato, X. Li, H.P. Hratchian, A.F. Izmaylov, J. Bloino, G. Zheng, J.L. Sonnenberg, M. Hada, M. Ehara, K. Toyota, R. Fukuda, J. Hasegawa, M. Ishida, T. Nakajima, Y. Honda, O. Kitao, H. Nakai, T. Vreven, J.A. Montgomery, Jr., J.E. Peralta, F. Ogliaro, M. Bearpark, J.J. Heyd, E. Brothers, K.N. Kudin, V.N. Staroverov, T. Keith, R. Kobayashi, J. Normand, K. Raghavachari, A. Rendell, J.C. Burant, S.S. Iyengar, J. Tomasi, M. Cossi, N. Rega, J.M. Millam, M. Klene, J.E. Knox, J.B. Cross, V. Bakken, C. Adamo, J. Jaramillo, R. Gomperts, R.E. Stratmann, O. Yazyev, A.J. Austin, R. Cammi, C. Pomelli, J.W. Ochterski, R.L. Martin, K. Morokuma, V.G. Zakrzewski, G.A. Voth, P. Salvador, J.J. Dannenberg, S. Dapprich, A.D. Daniels, O. Farkas, J.B. Foresman, J.V. Ortiz, J. Cioslowski, D.J. Fox, Gaussian, Inc., Wallingford CT, 2010.
- [54] J.B. Foresman, Pittsburg, PA, in: E. Frisch (Ed.). *Exploring Chemistry with Electronic Structure Methods: A Guide to Using Gaussian*, 1996.
- [55] R. Dennington, T. Keith, J. Millam, Gaussview, Version 5, Semichem Inc., Shawnee Mission, KS, 2009.
- [56] J.M.L. Martin, C. Van Alsenoy, GAR2PED, a Program to Obtain a Potential Energy Distribution from a Gaussian Archive Record, University of Antwerp, Belgium, 2007.
- [57] T. Lu, F. Chen, Multiwfn: a multifunctional wavefunction analyzer, *J. Comput. Chem.* 33(2012) 580-592.
- [58] T. Lu, F. Chen, Quantitative analysis of molecular surface based on improved Marching Tetrahedra algorithm, *J. Mol. Graph. Model.* 38 (2012) 314-323.
- [59] L. Tian, C. Feiwu, Calculation of molecular orbital composition, *Acta Chim. Sinica* 69 (2011) 2393-2406.

- [60] M. Xiao, T. Lu, Generalized Charge Decomposition Analysis (GCDA) Method, *J. Adv. Phys. Chem.* 4 (2015) 111-124 (in Chinese)
- [61] W. Humphrey, A. Dalke, K. Schulten, VMD: visual molecular dynamics *J. Mol. Graph.* 14 (1996) 33-38.
- [62] J.E. Stone, J. Gullingsrud, K. Schulten. *A system for interactive molecular dynamics simulation.* in *Proceedings of the 2001 symposium on Interactive 3D graphics.* 2001. ACM.
- [63] J. Eargle, D. Wright, Z. Luthey-Schulten, Multiple Alignment of protein structures and sequences for VMD, *Bioinformatics* 22 (2006) 504-506.
- [64] D. Frishman, P. Argos, Knowledge-based protein secondary structure assignment, *Proteins.* 23 (1995) 566-579.
- [65] V. Amitabh, J. Frederick, P. Brooks, W.V. Wright, *Linearly Scalable Computation of Smooth Molecular Surfaces,* in *IEEE Computer Graphics and Applications.* 1994.
- [66] M.F. Sanner, A.J. Olson, J.-C. Spohner. *Fast and robust computation of molecular surfaces.* in *Proceedings of the eleventh annual symposium on Computational geometry.* 1995. ACM.
- [67] R. Sharma, M. Zeller, V.I. Pavlovic, T.S. Huang, Z. Lo, S. Chu, Y. Zhao, J.C. Phillips, K. Schulten, Speech/gesture interface to a visual-computing environment, *IEEE Comput. Graph.* 20 (2000) 29-37.
- [68] J.E. Stone, *An efficient library for parallel ray tracing and animation.* 1998.
- [69] A.S. El-Azab, K. Jalaja, A.A.M. Abdel-Aziz, A.M. Al-Obaid, Y.S. Mary, C.Y. Panicker, C. Van Alsenoy, Spectroscopic analysis (FT-IR, FT-Raman and NMR) and molecular docking study of 2-ethyl-(4-oxo-3-phenethyl-3,4-dihydroquinazolin-2-ylthio)-acetate, *J. Mol. Struct.* 1119 (2016) 451-461.
- [70] R.T. Ulahannan, C.Y. Panicker, H.T. Varghese, R. Musiol, J. Jampilek, C. Van Alsenoy, J.A. War, A.A. Al-Saadi, Vibrational spectroscopic and molecular docking study of (2E)-N-(4-chloro-2-oxo-1,2-dihydroquinolin-3-yl)-3-phenylprop-2-enamide, *Spectrochim. Acta* 151 (2015) 335-349.

- [71] J.B. Bhagyasree, J. Samuel, H.T. Varghese, C.Y. Panicker, M. Arisoy, O. Tempiz-Arpaci, Synthesis, FT-IR investigations and computational study of 5-[(4-bromophenyl)acetamido]-2-(4-tert-butylphenyl)benzoxazole, *Spectrochim. Acta* 115 (2013) 79-91.
- [72] Y.S. Mary, C.Y. Panicker, T.S. Yamuna, M.S. Siddegowda, H.S. Yathirajan, A.A. Al-Saadi, C. Van Alsenoy, Theoretical investigations on the molecular structure, vibrational spectra, HOMO-LUMO and NBO analysis of 9-[3-(dimethylamino) propyl]-2-trifluoromethyl-9H-thioxanthene-9-ol, *Spectrochim. Acta* 132 (2014) 491-501.
- [73] N.P.G. Roeges, *A Guide to the Complete Interpretation of Infrared Spectra of Organic Structures*, John Wiley and Sons Inc., New York, 1994.
- [74] N.B. Colthup, L.H. Daly, S.E. Wiberly, *Introduction of Infrared and Raman Spectroscopy*, Academic Press, New York, 1975.
- [75] G. Socrates, *Infrared Characteristic Group Frequencies*, John Wiley and Sons, New York, 1981.
- [76] S. Nigam, M.M. Patel, A. Ray, Normal coordinate analysis and CNDO/II calculations of isonitrosopropiophenone (propiophenone oxime) and its semicarbazone and thiosemicarbazone derivatives, synthesis and characterization of their metal complexes, *J. Phys. Chem. Solids*, 61 (2000) 1389-1398.
- [77] R.T. Ulahannan, C.Y. Panicker, H.T. Varghese, R. Musiol, J. Jampilek, C. Van Alsenoy, J.A. War, S.K. Srivastava, Molecular structure, FT-IR, FT-Raman, NBO, HOMO and LUMO, MEP, NLO and molecular docking study of 2-[(E)-2-(2-bromophenyl)ethenyl]quinoline-6-carboxylic acid, *Spectrochim. Acta* 151 (2015) 184-197.
- [78] H.T. Varghese, C.Y. Panicker, K.M. Pillai, Y.S. Mary, K. Raju, T.K. Manojkumar, A. Bielenca, C. Van Alsenoy, Spectroscopic investigations and computational study of 4-(3-bromophenyl)-4-azatricyclo[5.2.2.0.2,6]undecane-3,5,8-trione, *Spectrochim. Acta* 76 (2010) 513-522.
- [79] K.C. Mariamma, H.T. Varghese, C.Y. Panicker, K. John, J. Vinsova, C. Van Alsenoy, Vibrational spectroscopic investigations and computational study of 5-chloro-2-[4-(trifluoromethyl)phenylcarbamoyl]phenyl acetate, *Spectrochim. Acta* 112 (2013) 161-168.

- [80] T. Joseph, H.T. Varghese, C.Y. Panicker, K. Viswanathan, M. Dolezal, T.K. Manojkumar, C. Van Alsenoy, Vibrational spectroscopic investigations and computational study of 5-tert-butyl-N-(4-trifluoromethylphenyl)pyrazine-2-carboxamide, *Spectrochim. Acta* 113 (2013) 203-214.
- [81] G. Varsanyi, *Assignments of Vibrational Spectra of Seven Hundred Benzene Derivatives*, Wiley, New York, 1974.
- [82] R. Renjith, Y.S. Mary, C.Y. Panicker, H.T. Varghese, M. Pakosinska-Parys, C. Van Alsenoy, A.A. Al-Saadi, Spectroscopic (FT-IR, FT-Raman) investigations and quantum chemical calculations of 1,7,8,9-tetrachloro-10,10-dimethoxy-4-{3-[4-(3-methoxyphenyl)piperazin-1-yl]propyl}-4-azatricyclo[5.2.1.0<sup>2,6</sup>]dec-8-ene-3,5-dione, *Spectrochim. Acta* 129 (2014) 438-450.
- [83] K. Wolinski, J.F. Hinton, P. Pulay, Efficient implementation of the gauge independent atomic orbital method for NMR chemical shift calculations, *J. Am. Chem. Soc.* 112 (1990) 8251-8260.
- [84] S. Ahmad, S. Mathew, P.K. Verma, Laser Raman and FT-infrared spectra of 3,5-dinitrobenzoic acid, *Indian J. Pure Appl. Phys.* 30 (1992) 764-765.
- [85] Z. Liu, Y. Qu, M. Tan, H. Zhu, 5-bromosalicylic acid, *Acta Cryst. E* 60 (2004) o1310-o1311.
- [86] R.L. Martin, Natural transition orbitals, *J. Chem. Phys.* 118(2003) 4775-4777.
- [87] T. Le Bahers, C. Adamo, I. Ciofini, A qualitative index of spatial extent in charge-transfer excitations, *J. Chem. Theory. Comput.* 7(2011) 2498-2506.
- [88] C.A. Guido, P. Cortona, B. Mennucci, C. Adamo, On the metric of charge transfer molecular excitations: a simple chemical descriptor, *J. Chem. Theory. Comput.* 9(2013) 3118-3126.
- [89] C. Adant, M. Dupuis, J.L. Bredas, Ab initio study of the nonlinear optical properties of urea: Electron correlation and dispersion effects, *Int. J. Quantum. Chem.* 56 (1995) 497-507.
- [90] E. Koscienc, J. Sanetra, E. Gondek, B. Jarosz, I.V. Kityk, J. Ebothe, A.V. Kityk, Optical poling effect and optical absorption of cyan, ethylcarboxyl and tert-butyl derivatives of 1H-pyrazolo[3,4]quinoline, experiment and quantum chemical simulations, *Spectrochim. Acta* 61 (2005) 1933-1938.

- [91] G. Gece, The use of quantum chemical methods in corrosion sciences, *Corros. Sci.* 50 (2008) 2981-2922.
- [92] S.H.R. Sebastian, M.A. Al-Alshaikh, A.A. El-Emam, C.Y. Panicker, J. Zitko, M. Dolezal, C. Van Alsenoy, Spectroscopic, quantum chemical studies, Fukui functions, in vitro antiviral activity and molecular docking of 5-chloro-N-(3-nitrophenyl)pyrazine-2-carboxamide, *J. Mol. Struct.* 1119 (2016) 188-199.
- [93] R.G. Parr, R.G. Pearson, Absolute hardness: companion parameter to absolute electronegativity, *J. Am. Chem. Soc.* 105 (1983) 7512-7561.
- [94] E. Scrocco, J. Tomasi, Electronic molecular structure, reactivity and intermolecular forces, an euristic interpretation by means of electrostatic molecular potentials, *Adv. Quantum Chem.* 11 (1978) 115-193.
- [95] F.J. Luque, J.M. Lopez, M. Oroscó, Perspective on electrostatic interactions of a solute with a continuum, a direct utilization of ab initio molecular potentials for the prevision of solvent effects, *Theor. Chem. Acc.* 103 (2000) 343-345.
- [96] N. Okulik, A.H. Jubert, Theoretical analysis of the reactive sites of non-steroidal anti-inflammatory drugs, *Internet Electron. J. Mol. Des.* 4 (2005) 17-30.
- [97] P. Sjöberg, J.S. Murray, T. Brinck, P. Politzer, Average local ionization energies on the molecular surfaces of aromatic systems as guides to chemical reactivity, *Canadian J. Chem.* 68 (1990) 1440-1443.
- [98] P. Politzer, F. Abu-Awwad, J.S. Murray, Comparison of density functional and Hartree-Fock average local ionization energies on molecular surfaces, *Int. J. Quantum Chem.* 69 (1998) 607-613.
- [99] A. Michalak, F. De Proft, P. Geerlings, R. Nalewajski, Fukui functions from the relaxed Kohn-Sham orbitals, *J. Phys. Chem. A* 103 (1999) 762-771.
- [100] M. Li, *Organic chemistry of drug degradation*. 2012: Royal Society of Chemistry.
- [101] T. Andersson, A. Broo, E. Evertsson, Prediction of drug candidates sensitivity toward autoxidation: computational estimation of C-H dissociation energies of carbon centered radicals, *J. Pharm. Sci.* 103 (2014) 1949-1955.
- [102] J.S. Wright, H. Shadnia, L.L. Chepelev, Stability of carbon centered radicals, effect of functional groups on the energetic of addition of molecular oxygen, *J. Comput. Chem.* 30 (2009) 1016-1026.

- [103] Y-R.Luo, *Handbook of bond dissociation energies in organic compounds*. 2002: CRC press.
- [104] G.Gryn'ova, J.L.Hodgson, M.L.Coote, Revising the mechanism of polymer autooxidation, *Org. Biomol. Chem.* 9 (2011) 480-490.
- [105] R.V. Vaz, J.R. Gomes, C.M. Silva, Molecular dynamics simulation of diffusion coefficients and structural properties of ketones in supercritical CO<sub>2</sub> at infinite dilution, *J. Supercritic. Fluids* 107 (2016) 630-638.
- [106] J.A. Martinez-Perez, S. Iyengar, H.E. Shannon, D. Bleakman, A. Alt, D.K. Clawson, B.M. Arnold, M.G. Bell, T.J. Bleisch, A.M. Castano, M. Del Prado, E. Dominguez, A.M. Escribano, S.A. Filla, K.H. Ho, K.J. Hudziak, C.K. Jones, A. Mateo, B.M. Mathes, E.L. Mattiuz, A.M. Ogden, R.M. Simmons, D.R. Stack, R.E. Stratford, M.A. Winter, Z. Wu, P.L. Ornstein, GluK1 antagonists from 6-(tetrazolyl)phenyl decahydroisoquinoline derivatives, in vitro profile and in vivo analgesic efficacy, *Bioorg. Med. ChemLett.* 23 (2013) 6463-6466.
- [107] A. Gupta, P. Mishra, S. K. Kashaw, V. Jatav, Synthesis, anticonvulsant, antimicrobial and analgesic activity of novel 1,2,4-dithiazoles, *Indian J. Pharm. Sci.* 70 (2008) 535-538.
- [108] V. Alagarsamy, G. Muruganathan, R. Venkateshperumal, Synthesis, analgesic, anti-inflammatory and antibacterial activities of some novel 2-methyl-3-substituted quinazolin-4-(3H)-ones, *Biol. Pharm. Bull.* 26 (2003) 1711-1714.
- [109] O. Trott, A. J. Olson, AutoDockVina: Improving the speed and accuracy of docking with a new scoring function, efficient optimization and multithreading, *J. Comput. Chem.* 31 (2010) 455-461.
- [110] B. Kramer, M. Rarey, T. Lengauer, Evaluation of the FlexX incremental construction algorithm for protein ligand docking, *PROTEINS: Struct. Funct. Genet.* 37 (1999) 228-241.

### Highlights

- A new thiourea derivative has been synthesized and investigated
- Experimental spectroscopic characterization has been compared with DFT calculations
- Global and local reactivity and charge transfer properties have been investigated
- Docking study suggests the title compound could act as an analgesic drug.